

Surface femtochemistry of CO/O₂/Pt(111): The importance of nonthermalized substrate electrons

Tsing-Hua Her, Richard J. Finlay, Claudia Wu, Eric Mazur

Gordon McKay Laboratory, Harvard University, 9 Oxford Street, Cambridge, MA 02138

We studied the surface femtochemistry of CO/O₂/Pt(111) induced with 0.3-ps laser pulses over a wide range of wavelength and fluence. Below 10 $\mu\text{J}/\text{mm}^2$, the yields depend linearly on fluence. Above 10 $\mu\text{J}/\text{mm}^2$, the yields scale nonlinearly in the fluence. From the dependence of the yields on wavelength, we determine that the nonlinear surface femtochemistry is influenced by nonthermal substrate electrons.

I. INTRODUCTION

It has been well-established that high-intensity subpicosecond laser pulses induce reactions among adsorbates on a metal surface by photo-excitation of electrons in the metal substrate.¹⁻⁵ There is an active debate, however, about the energy distribution of the electrons responsible for the reaction between adsorbates on a metal surface. According to one proposal, the adsorbates interact with an essentially thermal substrate electron distribution.⁶ Another proposal is that the photon-energy-dependent electron distribution plays a significant role in the surface reactions.⁴

We measured the desorption of O₂ and production of CO₂ from CO/O₂/Pt(111) induced with 0.3-ps laser pulses at 267, 400, and 800 nm to determine the dependence of the chemical reaction on the electron distribution. We find that the reaction is sensitive to photon energy and therefore we favor excitation of the adsorbates by nonthermal substrate electrons.

The yields in subpicosecond photo-induced reactions have a nonlinear dependence on fluence, a high quantum efficiency, highly-excited nonthermal internal-state distributions, and increasing translational energy with increasing laser fluence.^{1,3,4,6-11} Two-pulse correlation experiments show that the excitation has a lifetime of about 1 ps.^{4,10-13} Time-resolved surface second-harmonic generation indicates that desorption of CO from CO/Cu(111) is complete in less than 325 fs.⁸

When the photochemistry of CO/O₂/Pt(111) is induced with continuous light^{14,15} or nanosecond pulses,³ the yields of O₂ and CO₂ scale linearly with fluence and depend strongly on photon energy. We previously reported the first data on the transition from a linear to a nonlinear fluence-dependence under 267-nm pulse excitation,¹⁰ later confirmed using laser pulses at 310 nm⁶. Here we report observations of this transition at 267 nm and at 400 nm.

II. EXPERIMENT

We studied the photochemistry of CO/O₂/Pt(111) using laser pulses from a 1-kHz regeneratively-amplified Ti:sapphire laser. The 100-fs, 800-nm pulses are frequency-doubled in a 1-mm thick lithium barium borate crystal and frequency-tripled in a 0.3-mm thick beta-barium borate crystal. The laser pulse energy is varied with a waveplate and a polarizing beam splitter. The 267- and 400-nm pulses have 0.26- and 0.3-ps duration, respectively. The 800-nm pulses are chirped to 0.3 ps so the pulse durations at all wavelengths are similar.

The energy of each laser pulse is measured with a photodiode that is calibrated with a power meter. The response of the power meter varies less than 3% over the range 267–800 nm. To ensure that there is no nonlinear absorption in the platinum, we measured the fraction of the laser pulse energy absorbed into platinum. The measured absorption of the platinum is constant over the range of fluences used in the experiments, and is in agreement with the reflectivity calculated from the published dielectric function of platinum.¹⁶ We also verified that the absorption of the chamber window does not depend on fluence. These results confirm that the laser energy absorbed in the platinum is a constant fraction of the pulse energy measured outside the vacuum chamber.

The spatial profile of the laser pulses is measured with an ultraviolet-sensitive CCD camera. The profile captured by the camera is fit well by a Gaussian function. The fluence incident on the camera is reduced to a level where the camera response is linear by reflecting the beam off the front surfaces of two pieces of glass and is further attenuated with neutral-density filters. To confirm the accuracy of the camera-based spatial profile measurement, we measured the spatial profile of a Helium-Neon laser with the camera and compared it with the profile determined by scanning a pinhole through the beam while measuring the transmitted light with a photodiode. The camera and pinhole methods yield laser profiles that are identical to within 1%.

The absorbed laser fluence is determined from the energy absorbed in the platinum, and the spatial profile of the laser pulse, accounting for the 45° angle of incidence. The fluence varies over the profile of the laser spot; values quoted below refer to the absorbed fluence at the peak of the spatial profile. The tests described above confirm that there is no wavelength-dependent, nor any fluence-dependent systematic error in the calculation of absorbed fluence.

The experiments are conducted on a 12-mm diameter Pt(111) crystal in an ultrahigh vacuum chamber with a base pressure of 5×10^{-11} torr. All experiments are performed at a base temperature of 84 K. The crystal is cleaned using Ne ion sputtering at an ion energy of 500 eV, annealing in vacuum at 1100 K, and annealing in 10^{-8} torr oxygen at 500–1000 K.¹⁷ Surface order is verified with low-energy electron diffraction and surface cleanliness is verified with Auger spectroscopy.¹⁸

After cleaning, molecular oxygen and carbon monoxide are adsorbed to saturation on the platinum surface.^{15,19} Molecular oxygen is deposited on the platinum surface as soon as the temperature has fallen below 94 K after a cleaning cycle. Carbon monoxide is deposited after the oxygen. To reduce background pressure, all adsorbates are deposited using a tube of 12-mm diameter brought to within 3 mm of the platinum surface.

The laser-induced O_2 desorption yield and CO_2 reaction yield are measured with a quadrupole mass spectrometer operating in pulse-counting mode. We alternate between detecting O_2 and CO_2 on successive laser shots. Between shots, we translate the sample to an unirradiated part of the sample preparation. A potential difference of -90 V is applied between the sample and the ionizer of the mass spectrometer to prevent stray electrons interacting with the sample. A tube of 4-mm inner diameter extends from the ionizer to the sample. This tube collects molecules desorbed from the surface within 14° of the surface normal. The ionizer is enclosed in mesh to allow the laser-induced desorption and reaction products to escape. Using a high-speed mechanical shutter, we reduce the laser repetition

rate to allow the gas-phase products to be pumped out of the chamber between successive laser shots.

The yield depends on the area of the sample preparation exposed to the laser pulses. To obtain an appreciable yield at low fluence, a large laser spatial profile of full-width-half-maximum up to 1 mm² is used. At high fluence, the spatial profile is decreased to as low as 0.05 mm² to reduce the absolute yield and avoid saturating the pulse-counting electronics. The yields reported below are divided by the laser spot size to allow comparison between runs taken with different laser spot sizes. Below 20 μJ/mm², less than 1% of the adsorbates is depleted by a single laser pulse; to increase the signal in this regime, we admit up to 10 pulses at a 1-kHz rate to one spot on the sample and the mass spectrometer measures the total yield.

III. RESULTS

Figure 1 shows the yield of oxygen molecules obtained from CO/O₂/Pt(111) with 267-, 400-, and 800-nm laser pulses. Around 10 μJ/mm² there is a clear change in the dependence of the yield on absorbed laser fluence. Above 50 μJ/mm², the yield saturates because the pulse desorbs an appreciable fraction of the adsorbed oxygen.⁴

Below 10 μJ/mm² the yield from 267- and 400-nm pulses depends linearly on fluence. To determine the linear cross section in this regime, we measured the decreasing yield from a single spot on the sample as the surface coverage is depleted by 3,000 laser pulses. The linear cross sections thus obtained are $\sigma_{267} = (4 \pm 2) \times 10^{-19} \text{ cm}^2$ and $\sigma_{400} = (4 \pm 2) \times 10^{-20} \text{ cm}^2$ for 267- and 400-nm pulses, respectively. We do not observe any linear dependence of yield on fluence for 800-nm laser pulses; continuous light sources with wavelengths longer than 600 nm also do not induce reaction¹⁵.

Between 10 and 50 μJ/mm² the yield depends nonlinearly on fluence. The data can be described by a simple power law, $Y_0 \sim F^p$, where $p > 1$ and F is the fluence absorbed in the platinum. As Table 1 shows, the exponent p decreases with decreasing wavelength.

The wavelength dependence of the yields is also apparent in a comparison of the absolute yields at a particular fluence. Table 2 summarizes the wavelength dependence of the yields at 1 and 30 $\mu\text{J}/\text{mm}^2$. At both fluences, the yield increases substantially as the wavelength decreases.

Figure 2 shows the yield of carbon dioxide from the same sample preparation as Figure 1. The dependence of the CO_2 yield on fluence is similar to that of O_2 . Table 3 summarizes the ratio of yield of O_2 to yield of CO_2 . When using 267- or 400-nm pulses at fluences below 10 $\mu\text{J}/\text{mm}^2$ (*i.e.*, in the linear regime), the yields of O_2 and CO_2 are the same. Above 20 $\mu\text{J}/\text{mm}^2$, the yield of O_2 is substantially more than the yield of CO_2 , and the ratio is smaller at shorter wavelengths. The ratios shown in Table 3 are not corrected for the small dependence of the mass spectrometer detection efficiency on species.

IV. DISCUSSION

The desorption and reaction yields at fluences below 10 $\mu\text{J}/\text{mm}^2$, shown in Figures 1 and 2, scale linearly in fluence. The cross sections are in the range of 10^{-19} and increase with decreasing wavelength. The yield of O_2 and CO_2 obtained from $\text{CO}/\text{O}_2/\text{Pt}(111)$ with continuous light¹⁵ or nanosecond-pulses³ also scales linearly in fluence. The cross sections measured with these low-intensity sources are in the range of 10^{-19} cm^2 and increase with decreasing wavelength. We therefore attribute the linear surface femtochemistry to the same mechanism responsible for the surface photochemistry induced with continuous-wave or nanosecond-pulsed light sources.

The excitation of $\text{CO}/\text{O}_2/\text{Pt}(111)$ under irradiation with these low-intensity sources has been attributed to electronic transitions into normally-vacant orbitals of the O_2 .¹⁵ This new electronic configuration causes the adsorbate atoms to move, accumulating vibrational or translational energy that may lead to desorption or reaction. Two mechanisms for the electronic transition have been proposed. The photon can stimulate a direct transition between orbitals in the $\text{O}_2/\text{Pt}(111)$ complex.¹⁵ Alternatively, the photon may excite an electron to a state above the Fermi level in the $\text{Pt}(111)$ band structure, from which it crosses

into an orbital of the O₂/Pt(111) complex.²⁰ Either way, the electron interacts with the O₂ while retaining a substantial portion of the initial photon energy. The surface photochemistry in the linear regime is therefore governed by electrons with a nonthermal distribution. The wavelength dependence of the cross section is due to the required matching of the energy of the photo-excited electron with the energies of the vacant O₂ orbitals.

Irradiation of a metal surface creates an electron distribution with thermal and nonthermal components. For intense subpicosecond laser pulses, the thermal distribution of electrons can reach several thousand Kelvin for a few picoseconds.¹ Several authors attributed the nonlinear dependence of yield on fluence, high desorption yields, and short excitation lifetimes to these transient hot electrons.^{9,21-23} The electron temperature depends on the pulse duration and the fluence absorbed in the platinum, but not on photon wavelength.²⁴

Our experiments show three ways in which the nonlinear surface femtochemistry depends on wavelength. The power-law exponents summarized in Table 1 depend on wavelength, increasing from 4.8 ± 0.5 at 267 nm to 7.2 ± 0.5 at 800 nm. The desorption yields summarized in Table 2 are also wavelength dependent: at $30 \mu\text{J}/\text{mm}^2$, the yield from 267-nm pulses is about 4 times that from 400-nm pulses, and about 65 times that from 800-nm pulses. The ratio between O₂ and CO₂ yields, summarized in Table 3, depends on wavelength, varying from 70 at 800 nm to 25 at 267 nm. The nonlinear femtochemistry of CO/O₂/Pt(111) depends on wavelength, and so the thermalized electron distribution cannot be solely responsible for exciting the adsorbates. We attribute the wavelength dependence of the nonlinear surface femtochemistry on CO/O₂/Pt(111) to interaction of the adsorbates with electrons from a nonthermal distribution.

Several authors have measured the yield of O₂ from O₂/Pt(111) obtained with two high-fluence subpicosecond laser pulses incident on the same spot on the sample with a variable delay between the pulses.^{4,13} The dependence of the yield on delay indicates that

the sample retains memory of the excitation for about 1 ps.⁴ Several authors have measured the time over which a nonthermal electron distribution persists in a gold film following subpicosecond laser-excitation. In gold, electron thermalization can take about 0.5 ps.^{25,26} Though there are no published measurements for platinum, the electron thermalization time in platinum is likely less than the observed two-pulse correlation time in desorption of O₂ from O₂/Pt(111). The correlation time could reflect the time required for the adsorbates to dissipate the vibrational excitation induced by the first laser pulse. Alternatively, it could indicate that the O₂ desorption is also influenced by the transiently hot thermalized electrons, which cool on this timescale.

There are practical benefits to being able to access two different femtochemistry regimes. At high fluence, where desorption is more efficient than reaction, adsorbates can be desorbed with subpicosecond time-resolution for analysis. The efficient desorption could also be used to create empty reactive sites and increase reaction rate in a catalytic process in which site blocking inhibits the reaction. Finally, because the linear surface femtochemistry is caused by the same mechanism as the surface photochemistry induced with continuous light, the dynamics of the surface photochemistry induced with continuous light can be studied with femtosecond time-resolution by limiting the femtosecond pulses to low fluence.

The transition between nonlinear and linear surface femtochemistry is also of theoretical interest. At low fluence, the linear dependence of yield on fluence is due to desorption or reaction caused by a single electronic excitation. Above the transition fluence, the nonlinearity indicates that cooperative action of the photo-excited electrons dominates the linear process. These cooperative effects have been described as a frictional coupling between the substrate electrons and the adsorbates,²² and as a repeated excitation of the adsorbate within the time required for cooling of the adsorbate vibration²³.

In conclusion, we describe the surface femtochemistry of O₂/CO/Pt(111) as follows. Linear surface femtochemistry, observed at fluences below 10 $\mu\text{J}/\text{mm}^2$, is due to the same

mechanism as surface photochemistry induced with continuous wave and nanosecond pulses. Above $10 \mu\text{J}/\text{mm}^2$, another excitation mechanism dominates the reaction; yields are nonlinear in fluence and depend on wavelength. At all fluences the adsorbates are stimulated by nonthermal electrons. Models need to account for the nonthermal electrons to predict the wavelength dependence of our data.

ACKNOWLEDGEMENTS

We wish to thank Professors Cynthia Friend and Eric Heller for many valuable discussions. This work was supported by the Army Research Office grants DAAH04-95-0615 and DAAH04-95-0370. RJF acknowledges a scholarship from the Natural Science and Engineering Research Council of Canada. CW gratefully acknowledges a graduate fellowship from the Cusanuswerk.

- 1 J.A. Prybyla, T.F. Heinz, J.A. Misewich, M.M.T. Loy, and J.H. Glownia, *Phys. Rev. Lett.* **64**, 1537-1540 (1990).
- 2 F. Budde, T.F. Heinz, M.M.T. Loy, J.A. Misewich, F. de Rougemont, and H. Zacharias, *Phys. Rev. Lett.* **66**, 3024-3027 (1991).
- 3 F.-J. Kao, D. G. Busch, D. Gomes da Costa, and W. Ho, *Phys. Rev. Lett.* **70**, 4098-4101 (1993).
- 4 S. Deliwala, R.J. Finlay, J.R. Goldman, T.H. Her, W.D. Miehler, and E. Mazur, *Chem. Phys. Lett.* **242**, 617-622 (1995).
- 5 R.J. Finlay, T.-H. Her, C. Wu, and E. Mazur, *Chem. Phys. Lett.* **274**, 499-504 (1997).
- 6 D.G. Busch and W. Ho, *Phys. Rev. Lett.* **77**, 1338-1341 (1996).
- 7 F. Budde, T.F. Heinz, A. Kalamarides, M.M.T. Loy, and J.A. Misewich, *Surf. Sci.* **283**, 143-157 (1993).
- 8 J.A. Prybyla, H.W.K. Tom, and G.D. Aumiller, *Phys. Rev. Lett.* **68**, 503-506 (1992).
- 9 Lisa M. Struck, Lee J. Richter, Steven A. Buntin, Richard R. Cavanagh, and John C. Stephenson, *Phys. Rev. Lett.* **77**, 4576-4579 (1996).
- 10 R.J. Finlay, S. Deliwala, J.R. Goldman, T.H. Her, W.D. Miehler, C. Wu, and E. Mazur, in *Proceedings of the SPIE - Laser Techniques for Surface Science II* (1995), Vol. 2547, pp. 218-226.
- 11 J.A. Misewich, A. Kalamarides, T.F. Heinz, U. Höfer, and M.M.T. Loy, *J. Chem. Phys.* **100**, 736-739 (1994).
- 12 D.G. Busch, Shiwu Gao, R.A. Pelak, M.F. Booth, and W. Ho, *Phys. Rev. Lett.* **75**, 673-676 (1995).

- 13 F.-J. Kao, D. G. Busch, D. Cohen, D. Gomes da Costa, and W. Ho, *Phys. Rev. Lett.* **71**, 2094-2097 (1993).
- 14 X.-Y. Zhu, S. R. Hatch, A. Campion, and J.M. White, *J. Chem. Phys.* **91**, 5011-5020 (1989).
- 15 W.D. Mieher and W. Ho, *J. Chem. Phys.* **99**, 9279-9295 (1993).
- 16 J. H. Weaver, C. Krafka, D. W. Lynch, and E. E. Koch, *Optical Constants of Materials, Part I, Physics Data* (1981).
- 17 R.G. Musket, W. McLean, C.A. Colmenares, D.M. Makowiecki, and W.J. Siekhaus, *Applications of Surf. Sci.* **10**, 143-207 (1982).
- 18 C. Emil Tripa, Christopher R. Arumaninayagam, and John T. Yates, *J. Chem. Phys.* **105**, 1691-1696 (1996).
- 19 John Gland, Vrett Serton, and Galen Fisher, *Surface Science* **95**, 587-602 (1980).
- 20 F. Weik, A. de Meijere, and E. Hasselbrink, *J. Chem. Phys.* **99**, 682 (1993).
- 21 W. Ho, *Surf. Sci.* **363**, 166-178 (1996).
- 22 Clayton Springer and Martin Head-Gordon, *Chem. Phys.* **205**, 73-89 (1996).
- 23 J.A. Misewich, T.F. Heinz, and D.M. Newns, *Phys. Rev. Lett.* **68**, 3737-3740 (1992).
- 24 S. I. Anisimov, B. L. Kapeliovich, and T. L. Perel'man, *Sov. Phys. JETP* **39**, 375 (1974).
- 25 W.S. Fann, R. Storz, H.W.K. Tom, and J. Bokor, *Surf. Sci.* **283**, 221-225 (1993).
- 26 C. Suárez, W.E. Bron, and T. Juhasz, *Phys. Rev. Lett.* **75**, 4536-4539 (1995).

- Figure 1** Yields of O₂ from CO/O₂/Pt(111) obtained with laser pulses of 0.3-ps duration at ▲ 800-, ● 400-, and ■ 267-nm wavelengths.
- Figure 2** Yields of CO₂ from CO/O₂/Pt(111) obtained with laser pulses of 0.3-ps duration at △ 800-, ○ 400-, and □ 267-nm wavelengths.
- Table 1** Wavelength dependence of the power law exponent. The yield is linear in fluence below 10 μJ/mm², but very nonlinear in fluence above 10 μJ/mm². There is no low-fluence yield with 800-nm laser pulses.
- Table 2** Wavelength dependence of the laser-induced yield. At all fluences studied, the yield increases with decreasing wavelength.
- Table 3** Wavelength dependence of the ratio of O₂ to CO₂ yield. The ratio is one at fluences below 10 μJ/mm², but O₂ desorption is favored over production of CO₂ at fluences above 20 μJ/mm². At fluences above 20 μJ/mm², the ratio is strongly wavelength dependent.

<i>F</i>	<i>p</i>		
	267 nm	400 nm	800 nm
$< 10 \mu\text{J}/\text{mm}^2$	1.1 ± 0.1	0.9 ± 0.1	–
$> 10 \mu\text{J}/\text{mm}^2$	4.8 ± 0.5	6.0 ± 0.5	7.2 ± 0.5

Table 1

<i>F</i>	<i>Y</i>		
	267 nm	400 nm	800 nm
$1 \mu\text{J}/\text{mm}^2$	3 ± 0.5	0.1 ± 0.02	0
$30 \mu\text{J}/\text{mm}^2$	8000 ± 1500	2000 ± 500	120 ± 25

Table 2

F	$Y_{O_2}:Y_{CO_2}$		
	267 nm	400 nm	800 nm
$< 10 \mu\text{J}/\text{mm}^2$	1 ± 0.1	1 ± 0.1	–
$> 20 \mu\text{J}/\text{mm}^2$	25 ± 5	55 ± 15	70 ± 10

Table 3

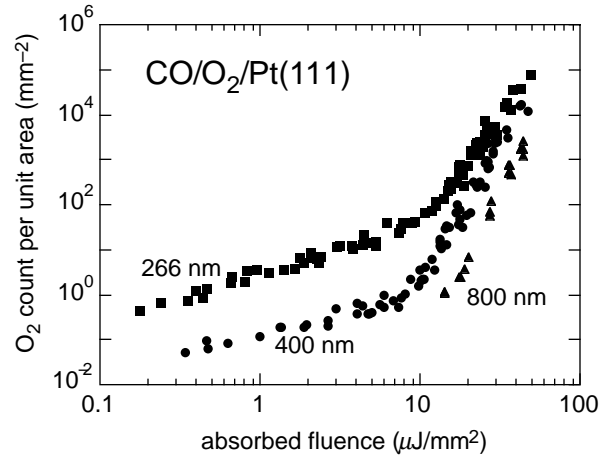


Figure 1

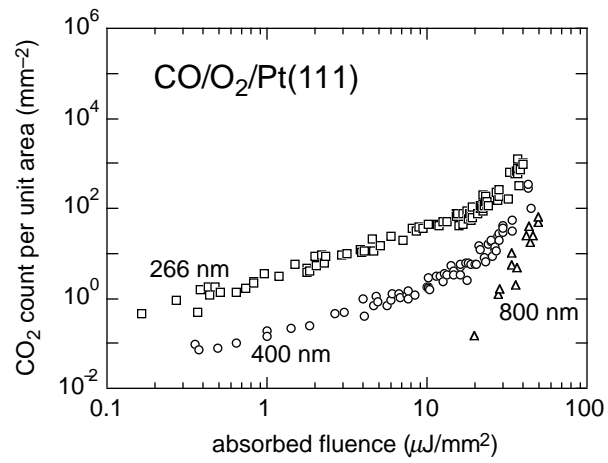


Figure 2